CHEMISTRY
A EUROPEAN JOURNAL

DOI: 10.1002/chem.201100563

Visual Scanometric Detection of DNA through Silver Enhancement Regulated by Gold-Nanoparticle Aggregation with a Molecular Beacon as the Trigger

Hanxu Ji,[a] Haifeng Dong,[a] Feng Yan,[b] Jianping Lei,[a] Ling Ding,[a] Wenchao Gao,[a] and Huangxian Ju*[a]

Abstract: A convenient and label-free scanometric approach for DNA assay was designed by integrating a metal-ion-mediated conformational molecular beacon (MB) and silver-signal amplification regulated by gold-nanoparticle (AuNP) aggregation. The strategy was based on displacing the interaction between the target DNA sequence and a competitor Hg^{2+} ion with a link DNA sequence. In the absence of the target DNA sequence, a link DNA sequence interacted with the Hg^{2+} ions, thus forming an inactive cyclic conformation of the MB. This result led to the poor aggregation of polyadenosine-functionalized AuNPs (A-AuNP). In the presence of a target DNA sequence with a stronger affinity than that of the competitor, hybridization between the link DNA and target DNA sequences turned on the trigger. The polythymidine end of the resulting linear duplex structure could react with A-AuNP, thus leading to a cross-linking aggregation. This aggregation weakened AuNP-catalyzed silver enhancement on a spot substrate. Further, by using scanometric detection, the concentration of the target DNA sequence could be conveniently read out within a linear range from 1.0 to 30 nM. Interestingly, in the same amount of Hg^{2+} ions, one-base mismatched DNA showed only 22% of the relative gray-scale intensity for the target DNA sequence at the same concentration, thus indicating good specificity. The designed approach, with the help of the ion-mediated conformational MB, was simple, cost effective, adaptable, and convenient and provided significant potential applications in clinical analysis.

Keywords: DNA · gold nanoparticles · molecular beacons · scanometric detection · silver · sensors

Introduction

The detection of DNA sequences is critical in various fields, such as in the diagnosis of infections and genetic diseases and in environmental and forensic applications. Thus, many methods based on Raman scattering,[1] electrochemical detection,[2–5] colorimetry,[6–10] field-effect transistors,[11] photoluminescence,[12–15] and electrogenerated chemiluminescence[16,17] have been developed for the highly sensitive and selective detection of DNA molecules. Compared with the other methods, colorimetry has been demonstrated to have several significant advantages, such as having a visual readout and being low cost, rapid to use, and easy to operate. Especially, metal-nanoparticle-based homogeneous colorimetry shows very promising applications in the detection of DNA sequences.[18,19] For example, colorimetric DNA detection that couples metallic nanoparticles was started by Mirkin and co-workers with the use of capture DNA-functionalized gold nanoparticles (AuNPs).[20] The intensive red color allowed the AuNPs to be used as a colorimetric label for DNA detection in a spot test. Furthermore, a colorimetric assay based on biobarcode amplification, magnetic separation, and the aggregation of DNA-modified AuNPs was proposed for the quantification of DNA by using a graphic processing method.[21] A homogeneous colorimetric DNA biosensor was also developed by a nicking endonuclease-assisted nanoparticle amplification process with a 103-fold improvement in amplification.[22] These studies usually use a DNA sandwich structure to detect the target DNA sequence. Herein, a conformational molecular beacon (MB), which was formed during the detection process by the specific interaction of thymine with a mercury ion, was introduced in the detection of the target DNA sequence to provide an efficient method for the selective visual detection of a MB-related target analyte.

A MB is a single-stranded DNA probe with a stem-loop structure. Recently, MBs have received considerable interest because of the inherent signaling mechanism by energy transfer and the high selectivity in the detection of DNA sequences and proteins.[22–27] Different from regular MBs that contain stems based on the Watson–Crick system, MBs based on a non-Watson–Crick system show greater selectivity, control, and resistance toward nuclease digestion than

[a] H. Ji, H. Dong, Dr. J. Lei, Dr. L. Ding, W. Gao, Prof. H. Ju
State Key Laboratory of Analytical Chemistry for Life Science
School of Chemistry and Chemical Engineering
Nanjing University, Nanjing 210093 (P.R. China)
Fax: (+86) 25-8359-3593
E-mail: hxju@nju.edu.cn

[b] F. Yan
Jiangsu Institute of Cancer Prevention and Cure
Nanjing 210009 (P.R. China)

common MBs.[28–30] The thermodynamic and kinetic features of a non-Watson–Crick MB can be conveniently modulated by independently varying the concentration of the metal ion and/or metal-ion-stablized MB. Therefore, the high specificity of interaction of oligonucleotides with metal ions makes them not only tools for the detection of metal ions by AuNP-enhanced surface plasmon resonance and photoluminescence,[31,32] but also suitable for use in the design of alternative approaches for the detection of amino acids,[33] DNA,[34] or redox environments[35] by colorimetric and fluorescent measurements.

A mercury ion was used in this study as a competitor of the target DNA sequence to form a thymidine-based MB (T-MB) and to develop a competitive method that involved the capture of DNA-functionalized AuNPs and amplification of silver deposits for the scanometric detection of DNA (Scheme 1). The scanometric technology involved a formation–recording procedure performed on a flatbed scanner. The readable signal came from a deposit formed on a substrate by an AuNP-catalyzed silver reduction reaction. At the beginning, in the absence of the target DNA sequence, a link DNA sequence interacted with the Hg^{2+} ions, thus forming an inactive cyclic conformation of the MB. This process led to poor aggregation of the polyadenosine-functionalized AuNP (A-AuNP), which catalyzed the silver reduction reaction by addition of the reducing reagent (e.g., hydroquinone) and produced a dark spot. On the contrary, in the presence of the target DNA sequence, hybridization between the target DNA and the link DNA sequences turned on the trigger due to stronger affinity of the target DNA sequence than that of the competitor Hg^{2+} ions. Afterward, the polythymidine end of the resulting linear duplex structure could react with the A-AuNP, thus leading to a cross-link aggregation, which resulted in a weakened silver deposition on the spot substrate. The extent of the silver enhancement depended proportionally on the concentration of the corresponding target DNA sequence. The metal-ion-mediated conformational MB provided a powerful visual tool to detect DNA sequences with high sensitivity and selectivity.

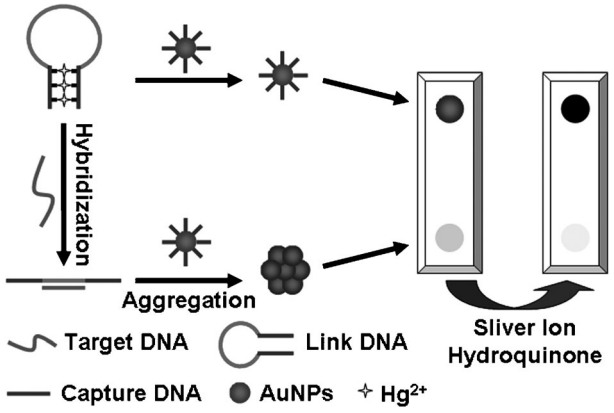

Scheme 1. Visual scanometric strategy for the detection of DNA with a molecular beacon as a trigger.

Results and Discussion

Characterization of AuNPs: Citrate-capped AuNPs were synthesized by the citrate reduction method.[36] A UV/Vis spectrum of AuNPs showed the absorption inflection point at $\lambda = 520$ nm, which was defined as the peak value to produce a diameter of 13 nm. This result was consistent with the observation from the high-resolution TEM image, in which a uniform size distribution of about 13 nm in diameter was observed. The concentration of AuNPs was determined to be 2.5 nM through an extinction coefficient of $\varepsilon = 2.7 \times 10^8\,M^{-1}cm^{-1}$ at $\lambda = 520$ nm for AuNPs with a diameter of 13 nm.

Fabrication and characterization of the spot substrate: The visualization and scanometric detection of the DNA-linked aggregation of A-AuNPs after silver enhancement was achieved on the spot substrate, which was characterized by measuring the contact-angle. The contact angles of the bare glass, glass treated with a piranha solution, and glass silanized with {3-[2-(2-aminoethyl)aminol]propyl}trimethoxysilane (AEPTS) were 41, 14, and 78°, respectively (Figure 1). The smaller contact angle of glass treated with a piranha solution than bare glass indicated its higher hydrophilicity (Figure 1 A, B). Furthermore, to obtain a well-defined A-AuNP spot, AEPTS was used to modify the glass slides for the preparation of the substrates, which led to a contact angle of 78° (Figure 1 C). After the A-AuNP solution (3 μL) was spotted on the substrate and left to stand at room temperature for 60 min to dry, the spot was immensely stable toward the washing in the silver enhancement procedure

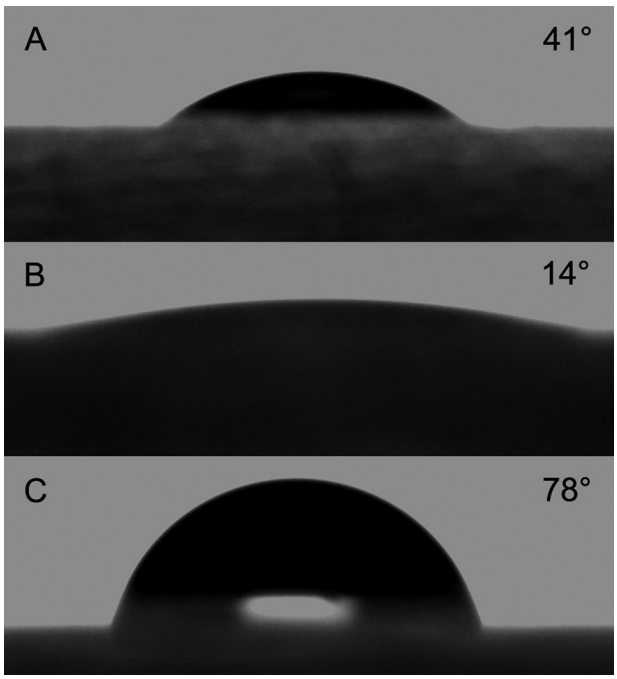

Figure 1. Contact angles of A) bare glass slide, B) the glass slide treated with a piranha solution, and C) the glass slide silanized with AEPTS.

owing to the interaction between the primary amine group in AEPTS and the A-AuNPs surface. The single short-strand oligonucleotide of capture DNA on A-AuNPs did not inhibit the interaction due to the controlled amount of capture DNA, which was calculated to regulate the aggregation of the AuNPs. Moreover, the substrate without spotting did not exhibit any background during the silver enhancement process.

Monitoring the DNA-linked aggregation of the AuNPs: The prepared A-AuNP solution was a stable red color, which is the characteristic color of dispersed AuNPs (Figure 2A, photo a). When the link DNA sequence was added to the AuNP solution, a purple color could be observed after 60 min at 4 °C owing to the blue-shifted plasmon band of the AuNPs (Figure 2A, photo b). This diagnostic feature of the aggregation process is well-understood. When different AuNPs came into proximity, the surface plasmon of the individual AuNPs combined, thus resulting in the change from red to blue.[19] However, in the absence of the link DNA sequence, the incubation of AuNPs with the target DNA sequence in the buffer did not show obvious change (Figure 2A, photo c). Therefore, the formation of the aggregate was attributed to the cross-linking AuNPs by the link DNA sequence.

This aggregation process could be easily and quickly visualized by combining aggregation-regulated silver-signal amplification with the spot test. The scanometric images of A-AuNPs treated with tris(hydroxymethyl)aminomethane (tris) buffer, the link DNA sequence, and the target DNA sequence are shown in Figure 2B. The A-AuNP solutions incubated with the link DNA sequence and tris buffer were spotted on an AEPTS-modified glass slide after mixing for 1 hour. After silver enhancements of 2×3 min, the color of the spots from the sample with the link DNA sequence (Figure 2B, photo b) was obviously lighter than the spots from the sample with only the tris buffer (Figure 2B, photo a), thus indicating the efficiency of the silver signal intensity as a signaling tool for the identification of the link DNA sequence. Furthermore, the silver-enhanced spot test greatly improved the sensitivity of the method and avoided the use of expensive apparatus. On the other hand, after the AuNP solution was incubated with the target DNA sequence and the spot was enhanced twice with silver deposition, a dark spot similar to that developed with the tris buffer was observed (Figure 2B, photo c), thus suggesting that the target DNA sequence did not lead to the aggregation of the A-AuNPs. Because only the exposed AuNPs could catalyze the reduction of the silver ions by hydroquinone to produce the silver staining spot,[37] the silver signal was closely related to the extent of the AuNP aggregation, which depended on the amount of the link DNA sequence present. Therefore, a scanometric approach to monitor the concentration of the link DNA sequence could be developed by a flatbed scanner associated with Adobe Photoshop.[21]

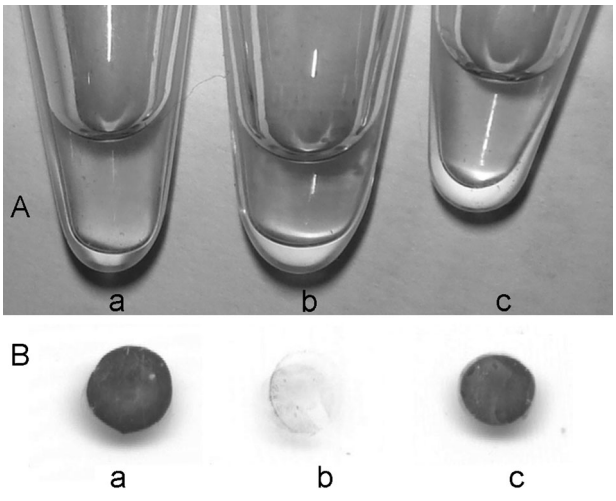

Figure 2. A) Photos and B) scanometric images of DNA–AuNPs treated with a) Tris buffer, b) the link DNA sequence, and c) the target DNA sequence.

In the presence of Hg^{2+} ions with a sufficient amount of the link DNA sequence in the solution, the incubation of the A-AuNP solution with the mixture followed by silver enhancement produced a scanometric image similar to Figure 2B (photos a and c, as shown in the first photo from right in Figure 3D) in the presence of excess Hg^{2+} ions. This outcome was due to the formation of T-MB by the interaction of the link DNA sequence with the Hg^{2+} ions, which turned off the hybridization of the link DNA sequence with the polyadenosine oligonucleotide on the A-AuNPs. Thus, the competition of the target DNA sequence with the Hg^{2+} ions to bind the link DNA sequence to form a linear duplex structure with a polythymidine end strand and the inactive

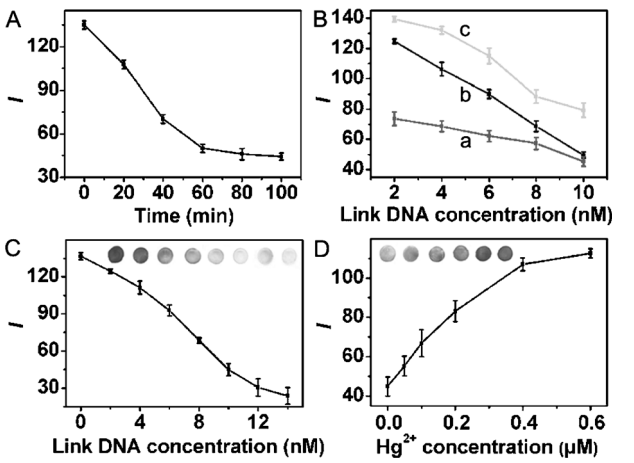

Figure 3. Dependence of *I* on the A) incubation time of the link DNA sequence at a concentration of 10 nM for aggregation with enhancements 2×; B) the concentration of the link DNA sequence for silver enhancements a) 1×, b) 2×, and c) 3×; C) the concentration of the link DNA sequence at enhancements 2× and scanometric images with the link DNA sequence at concentrations of at 0, 2, 4, 6, 8, 10, 12, and 14 nM (inset, from left to right); and D) the concentration of the Hg^{2+} ions with the concentration of the link DNA sequence at 10 nM and enhancements 2× and scanometric images at concentrations of the Hg^{2+} ions at 0, 0.05, 0.1, 0.2, 0.4, and 0.6 μM (inset, from left to right).

cyclic conformation of MB produced a signal related to the concentration of the target DNA sequence, thus leading to a specific detection method.

For convenient quantification of the target DNA sequence, the relative gray-scale intensity (I; calculated by subtracting the value of the gray-scale intensity of the spot from that of the background) was used to quantify the silver signal. A higher I value corresponds to a darker spot or stronger silver signal.

Optimization of the detection conditions: The experimental parameters, including the incubation time of the A-AuNPs with the link DNA sequence, silver-enhancement time, concentration of the link DNA sequence, and the concentration of Hg^{2+} ions, were optimized for obtaining a sensitive silver signal. The silver-enhancement process was regulated by AuNP aggregation upon the addition of the link DNA sequence, thus the aggregation time was first considered. With the increasing aggregation time, the silver signal weakened and the I value decreased because the increasing aggregation decreased the AuNP-catalyzed silver reduction reaction (Figure 3A). At the incubation time of 60 min, the plot of I versus incubation time trended to the minimum value and was therefore selected for the following assay.

The enhancement of the silver deposit could improve the signal. The silver enhancement was performed by repeating the silver deposition for 3 min. With the increasing total silver-enhancement time, due to the repetitions, the I value increased at the same concentration of the link DNA sequence (Figure 3B). However, a longer silver-enhancement time increased the background signals. By considering the high sensitivity and wide concentration range for the detection of the target DNA sequence, the maximum slope of the plot of I versus the concentration of the link DNA sequence was favorable. Thus, enhancements of 2×3 min were used to provide a linear correlation without sacrificing sensitivity (Figure 3B, curve b).

The images of spots showed a clear correlation between the darkness of the silver signal with the concentration of the link DNA sequence (Figure 3C). Under the conditions optimized above, the I value decreased with increasing concentration of the link DNA sequence and reached a plateau at 10 nM. The linear correlation range was determined to be between 2 and 10 nM. The silver signal was closely related to the aggregation of AuNPs, so the link DNA sequence had a sensitive influence on the aggregation of AuNPs and provided a convenient tool for detection in a DNA assay. By considering the good analytical performance demonstrated, the link DNA sequence was used at a concentration of 10 nM in the following measurements.

The recognition of Hg^{2+} ions by the link DNA sequence is shown in Figure 3D. With an increasing concentration of Hg^{2+} ions in tris acetate buffer containing the link DNA sequence (10 nM), the I value increased and reached a maximum value at 0.4 μM Hg^{2+} ions. The maximum I value was close to that obtained in the absence of the link DNA sequence (the first point in Figure 3C), thus suggesting that little cross-linking aggregation of the A-AuNPs occurred formed due to the formation of the T-Hg^{2+}-T structure and that Hg^{2+} ions at a concentration of 0.4 μM was sufficient to completely bind the link DNA sequence. Thus, Hg^{2+} ions at a concentration of 0.4 μM were added to the detection solution containing the target DNA sequence for scanometric detection.

DNA hybridization assay: Under the optimized conditions, the silver signal decreased linearly with the increasing concentration of the target DNA sequence and then reached a plateau at 30 nM (Figure 4A). At a signal of six times the standard deviation of the control, the limit of detection was 0.9 nM. The linear calibration range was 1–30 nM ($R=0.990$), which was similar to that of $\Delta\lambda=2$–30 nm by fluorescence detection with the use of a Hg^{2+}-mediated MB.[29] The visual readout of this scanometric method was low cost and rapid in the quantification of nucleic acids.

It is a useful feature that MBs can recognize their targets with higher specificity than linear single-strand DNA probes.[6] The specificity of the proposed scanometric method based on a non-Watson–Crick MB was examined by hybridization with a one-base mismatched DNA sequence and a non-complementary DNA sequence in the tris buffer at the same concentration as the target DNA sequence. The signal decreases in the I values that resulted from the one-base mismatched DNA sequence and the non-complementary DNA sequence were only 22 and 12%, respectively, in comparison with the target DNA sequence (Figure 4B). This outcome indicates a high specificity, which arose from the conformational constraint of the stem-loop structure of the MB. The presence of the stem made it thermodynamically unfavorable for the binding of the mismatched sequence to the loop.[28,29] Thus, the metal-ion-mediated conformational MB provided an efficient tool for the visual detection of the target with specificity.

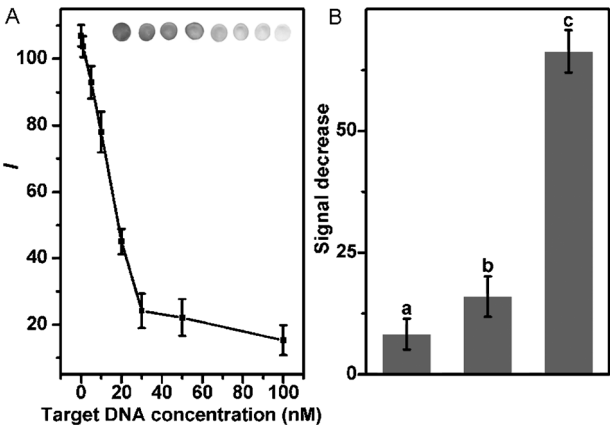

Figure 4. A) Plot of I versus the concentration of the target DNA sequence and scanometric images (inset) of the AuNPs incubated with the target DNA sequence at concentrations of 0, 1, 2, 5, 10, 30, 50 and 100 nM (from left to right) in Tris buffer containing 400 nM Hg^{2+} ions and 10 nM link DNA sequence; B) signal changes with a) 10 nM non-complementary DNA sequence, b) one-base mismatched DNA sequence, and c) the target DNA sequence.

To explore the applicability of the proposed strategy in realistically complex samples, the DNA sensor was used in the detection of a human-serum sample. Three droplets of the target DNA sequence, a one-base mismatched DNA sequence, and a non-complementary DNA sequence were dissolved respectively in a human-blood serum sample instead of tris buffer and the same analytical approach was performed. Compared with the individual results in tris buffer, the *I* values in the human serum sample decreased by 4, 7.3, and 7.1% for the target DNA sequence, one-base mismatched DNA sequence, and the non-complementary DNA sequence. These results indicate that the detection was unaffected by the human-blood sample, thus showing the good applicability of this strategy in real samples.

Conclusion

The efficient competitive binding of Hg^{2+} ions and a target DNA sequence to the polythymidine end of a link DNA sequence has been proven and results in the formation of a metal-ion-mediated MB and the decomposition of the MB. Thus, a facile and label-free scanometric approach for DNA assay has been developed by integrating a target-DNA-hybridized linear duplex structure with an exposed polythymidine end for A-AuNP aggregation and a AuNP-catalyzed silver deposition. This strategy provides a convenient and cost-effective analytical tool for analysis of nucleic acids with high specificity and a sensitivity similar to previously reported approaches that used fluorescence detection.[29] The metal-ion-mediated MB can be an efficient platform for monitoring the recognition of a corresponding target by the MB. This method has been proved particularly useful for rapid and simple point-mutation identification and can be extended to the selective visual detection of MB-related target analytes.

Experimental Section

Materials and reagents: Tris(2-carboxyethyl)phosphane hydrochloride (TCEP), tris(hydroxymethyl)aminomethane (tris), and a silver-enhancer kit including enhancement solutions A and B were purchased from Sigma–Aldrich (USA). {3-[2-(2-aminoethyl)aminol]propyl}trimethoxysilane (AEPTS) was purchased from Alfa Aesar China Ltd. $AuCl_3HCl{\cdot}4H_2O$ (>48% Au) and sodium citrate were obtained from the Shanghai Chemical Reagent Co., Ltd. (China). Tris acetate buffer (pH 8.2) contained tris buffer (0.025 mM), acetate (0.025 mM), and NaCl (100 mM). Ultrapure water was obtained from a Millipore water purification system (≥18 MΩ, Milli-Q, Millipore, Billerica, MA, USA) and was used in all the experiments. All the other reagents were of analytical grade and used without further purification. The oligonucleotides were purchased from Sangon Biological Engineering Technology & Co. Ltd. (Shanghai, China) and were purified using high-performance liquid chromatography (HPLC). Their sequences were expressed as follows:

link DNA sequence: 5′-TTTTTTTATGGGGTCT-GTCCGGTTCTGCTTGTTTTTTT-3′;

capture DNA 1: 3′-AAAAAAA-$(CH_2)_6$-SH-5′;

capture DNA 2: 5′-AAAAAAA-$(A)_{12}$-$(CH_2)_3$-SH-3′;

target DNA sequence: 5′-TGGAGCTACACCGACAACTCCA-3′;

one-base mismatched DNA: 5′-TGGAGCTACAGCGACAACTCCA-3′;

non-complementary DNA: 5′-GTGATCTCCGGACTTGACAATATC-3′.

Apparatus: The AuNPs were examined with a JEM 2100 high-resolution transmission electron microscope (HRTEM). UV/Vis absorption spectra were recorded on a UV-3600 UV/Vis/NIR photospectrometer (Shimadzu Co., Japan). The AuNP-spotted glass was scanned using an HP Scanjet 2400 scanner. The scanning parameters were highlights: 225; shadows: 6; midtones: 1.85. The static water contact angles were measured with a contact-angle system (OCA30, Dataphysics Instruments GmbH, Germany) using droplets of 1 μL of ultrapure water at 25°C.

Preparation of 5′- or 3′-(alkanethiol)oligonucleotide-modified AuNPs: Citrate-capped AuNPs (diameter: 13 nm) were prepared according to a reported protocol.[36] Trisodium citrate (5 mL, 1%) was added to a boiling solution of $HAuCl_4$ (200 mL, 0.01%). The solution changed from pale yellow to deep red within several minutes. The mixture was allowed to heat another several minutes to ensure complete reduction and was slowly cooled to room temperature with stirring. The A-AuNPs were synthesized according to a typical protocol.[38,39] Before DNA loading, the thiol functionality on the oligonucleotide probes was deprotected by treatment with 1.7 equivalents of TCEP for 1 h by using acetate buffer (0.05 M, pH 5.2) at room temperature. The AuNPs (3 mL, 2.5 nM) were functionalized with the deprotected thiololigonucleotides (capture DNA 1 or capture DNA 2; 10 μL, 100 μM, respectively) by incubation at room temperature for at least 16 h with gently stirring and an additional 24 h after the concentration of NaCl had been increased to 100 mM. These capture DNA-functionalized AuNPs were purified twice by centrifugation (17000 *g* for 25 min) in buffer containing NaCl (100 mM) and Tris acetate (25 mM, pH 8.2) and were dispersed in the Tris buffer.

Preparation of AEPTS-modified glass slides: The glass slides were first dipped in a piranha solution (hydrogen peroxide/sulfuric acid 30:70) for 12 h. After being washed thoroughly with water, they were dried under a stream of nitrogen and silanized by immersion in a solution of acetic acid (1 mM) containing AEPTS (1%) for 30 min at room temperature. After being rinsed with water and dried under a stream of nitrogen, the slides were baked for 30 min at 120°C.

DNA hybridization assay: The linked DNA (3 μL, 0.1 μM), Hg^{2+} ions (3 μL, 4.0 μM), and the target DNA sequence (3 μL) were mixed in a centrifuge tube. After the mixture was incubated for 30 min at room temperature, A-AuNPs (21 μL) containing AuNPs functionalized with capture DNA 1 and 2 mixed in a volume ratio of 1:1 was added to the mixture to react for another 60 min at 4°C. The spotting silver enhancement, scanning, and reading of the gray-scale intensity were performed by the following procedures:

An aliquot of the reaction mixture (3 μL) was transferred onto an AEPTS-modified glass slide to allow the adsorption of AuNPs over 1 h. After rinsing the slide with water, the silver enhancement was performed twice by immersing the slide in a 1:1 mixture of the silver enhancement solutions A and B for 3 min and then rinsing with water. For quantification of the extent of the aggregation of AuNPs, the slide was dried and scanned using a scanner, and the resulting image was quantified by reading the gray-scale intensity by using Adobe Photoshop software (0–256 for dark to the strongest intensity). Considering that a stronger silver signal showed a darker spot, which corresponded to a lower value of the gray-scale intensity, the relative gray-scale intensity *I* was used to quantify the silver signal of the spots by subtracting the value of the gray-scale intensity of the spot from that of the background. After this data processing, a stronger silver signal corresponded to a higher *I* value.

Acknowledgements

This study was financially supported by the Important National S&T Specific Project (2009ZX10004–313), the National Basic Research Program (2010CB732400), the National Natural Science Foundation of China (20875044, 20821063, 21075055), and the Natural Science Foundation of Jiangsu (BK2008014).

[1] J. D. Driskell, R. A. Tripp, *Chem. Commun.* **2010**, *46*, 3298–3300.
[2] H. F. Dong, F. Yan, H. X. Ji, D. K. Y. Wong, H. X. Ju, *Adv. Funct. Mater.* **2010**, *20*, 1173–1179.
[3] Y. W. Hu, T. Yang, X. X. Wang, K. Jiao, *Chem. Eur. J.* **2010**, *16*, 1992–1999.
[4] Z. P. Zhang, J. Y. Zhou, A. Tang, Z. Y. Wu, G. L. Shen, R. Q. Yu, *Biosens. Bioelectron.* **2010**, *25*, 1953–1957.
[5] H. Zhang, C. C. Fang, S. S. Zhang, *Chem. Eur. J.* **2010**, *16*, 12434–12439.
[6] Y. Y. Zhang, Z. W. Tang, J. Wang, H. Wu, A. H. Maham, Y. H. Lin, *Anal. Chem.* **2010**, *82*, 6440–6446.
[7] M. Hong, X. Zhou, Z. Q. Lu, J. Zhu, *Angew. Chem.* **2009**, *121*, 9667–9670; *Angew. Chem. Int. Ed.* **2009**, *48*, 9503–9506.
[8] J. Elbaz, M. Moshe, B. Shlyahovsky, I. Willner, *Chem. Eur. J.* **2009**, *15*, 3411–3418.
[9] Y. J. Song, X. H. Wang, C. Zhao, K. G. Qu, J. S. Ren, X. G. Qu, *Chem. Eur. J.* **2010**, *16*, 3617–3621.
[10] F. Xia, X. L. Zuo, R. Q. Yang, Y. Xiao, D. Kang, A. V. Bélisle, X. Gong, J. D. Yuen, B. B. Y. Hsu, A. J. Heeger, K. W. Plaxco, *Proc. Natl. Acad. Sci. USA* **2010**, *107*, 10837–10841.
[11] G. J. Zhang, Z. H. H. Luo, M. J. Huang, G. K. I. Tay, E. A. Lim, *Biosens. Bioelectron.* **2010**, *25*, 2447–2453.
[12] H. F. Dong, W. C. Gao, F. Yan, H. X. Ji, H. X. Ju, *Anal. Chem.* **2010**, *82*, 5511–5517.
[13] E. S. Jeng, J. D. Nelson, K. L. J. Prather, M. S. Strano, *Small* **2010**, *6*, 40–43.
[14] S. W. Bae, M. S. Cho, S. S. Hur, C. B. Chae, D. S. Chung, W. S. Yeo, J. I. Hong, *Chem. Eur. J.* **2010**, *16*, 11572–11575.
[15] X. Wang, X. H. Lou, Y. Wang, Q. C. Guo, Z. Fang, X. H. Zhong, H. J. Mao, Q. H. Jin, L. Wu, H. Zhao, J. L. Zhao, *Biosens. Bioelectron.* **2010**, *25*, 1934–1940.
[16] S. Cai, C. W. Lau, J. Z. Lu, *Anal. Chem.* **2010**, *82*, 7178–7184.
[17] Y. Chai, D. Y. Tian, W. Wang, H. Cui, *Chem. Commun.* **2010**, *46*, 7560–7562.
[18] L. Ding, R. C. Qian, Y. D. Xue, W. Cheng, H. X. Ju, *Anal. Chem.* **2010**, *82*, 5804–5809.
[19] W. A. Zhao, M. M. Ali, S. D. Aguirre, M. A. Brook, Y. F. Li, *Anal. Chem.* **2008**, *80*, 8431–8437.
[20] R. Elghanian, J. J. Storhoff, R. C. Mucic, R. L. Letsinger, C. A. Mirkin, *Science* **1997**, *277*, 1078–1081.
[21] J. M. Nam, K. J. Jang, J. T. Groves, *Nat. Protoc.* **2007**, *2*, 1438–1444.
[22] W. Xu, X. J. Xue, T. H. Li, H. Q. Zeng, X. G. Liu, *Angew. Chem.* **2009**, *121*, 6981–6984; *Angew. Chem. Int. Ed.* **2009**, *48*, 6849–6852.
[23] Y. C. Hara, T. G. Fujii, H. M. Kashida, K. J. Sekiguchi, X. G. Liang, K. S. Niwa, T. K. Takase, Y. S. Yoshida, H. Y. Asanuma, *Angew. Chem.* **2010**, *122*, 5634–5638; *Angew. Chem. Int. Ed.* **2010**, *49*, 5502–5506.
[24] Y. Xiao, X. H. Lou, T. K. Uzawa, K. J. I. Plakos, K. W. Plaxco, H. T. Soh, *J. Am. Chem. Soc.* **2009**, *131*, 15311–15316.
[25] E. Sharon, R. Freeman, I. Willner, *Anal. Chem.* **2010**, *82*, 7073–7077.
[26] H. Gong, T. Y. Zhong, L. Gao, X. H. Li, L. J. Bi, H. B. Kraatz, *Anal. Chem.* **2009**, *81*, 8639–8643.
[27] R. L. Stoermer, K. B. Cederquist, S. K. McFarland, M. Y. Sha, S. G. Penn, C. D. Keating, *J. Am. Chem. Soc.* **2006**, *128*, 16892–16903.
[28] R. H. Yang, J. Y. Jin, L. P. Long, Y. X. Wang, H. Wang, W. H. Tan, *Chem. Commun.* **2009**, 322–324.
[29] Y. W. Lin, H. T. Ho, C. C. Huang, H. T. Chang, *Nucleic Acids Res.* **2008**, *36*, e123.
[30] Y. X. Wang, J. S. Li, H. Wang, J. Y. Jin, J. H. Liu, K. M. Wang, W. H. Tan, R. H. Yang, *Anal. Chem.* **2010**, *82*, 6607–6612.
[31] L. Wang, T. Li, Y. Du, C. G. Chen, B. L. Li, M. Zhou, S. J. Dong, *Biosens. Bioelectron.* **2010**, *25*, 2622–2626.
[32] M. Kumar, P. Zhang, *Biosens. Bioelectron.* **2010**, *25*, 2431–2435.
[33] J. S. Lee, P. A. Ulmann, M. S. Han, C. A. Mirkin, *Nano Lett.* **2008**, *8*, 529–533.
[34] Y. X. Wang, J. S. Li, J. Y. Jin, H. Wang, H. X. Tang, R. H. Yang, K. M. Wang, *Anal. Chem.* **2009**, *81*, 9703–9709.
[35] Y. K. Miyake, A. K. Ono, *Tetrahedron Lett.* **2005**, *46*, 2441–2443.
[36] A. Ambrosi, M. T. Castañeda, A. J. Killard, M. R. Smyth, S. Alegret, A. Merkoçi, *Anal. Chem.* **2007**, *79*, 5232–5240.
[37] Z. Zhang, C. L. Chen, X. S. Zhao, *Electroanalysis* **2009**, *21*, 1316–1320.
[38] J. W. Liu, Y. Lu, *Angew. Chem.* **2006**, *118*, 96–100; *Angew. Chem. Int. Ed.* **2006**, *45*, 90–94.
[39] J. W. Liu, Y. Lu, *Nat. Protoc.* **2006**, *1*, 246–252.

Received: February 20, 2011
Published online: August 17, 2011

